

## Modeling of hydrodynamical and hydrophysical processes in the Aral Sea\*

V.I. Kuzin, E.N. Golubeva

### Introduction

The problem of the Aral Sea is an example of ecological hazards caused by the human activity. In the 1960-s, the intensive use of water from the Amu-Darya and the Syr-Darya for irrigation changed the water balance in the Aral Sea resulting in the excess the evaporation over the precipitation and the river runoff. In 1989, this caused separation of the Northern and the Central Aral basins, and in 2000, the connection of the Lazarev, the Vozrojdenija islands with the mainland and the formation of a single Peninsula separating the Western (deep) and the Eastern (shallow) basins with connection only in the Northern part. As a result, the Aral Sea level height decreased from 53 to 32.5 m (in the Baltic system), has lost 80 % of water volume and 60 % of the sea surface. The salinity increased from 10 to 68–70 g/l thus destroying the fishing industry. The ecological and social consequences are also dramatic. This work is done under the support of the INTAS Grant 01-0511-REBASOWS. Objectives of the research are as follows: forecasting the future Aral Sea water and salt balance under different scenarios of the water inflow to the Aral coastal zone; definition of a sustainable ecological profile of a closed water body and selection of a strategy of a possible ecosystem, biodiversity and bioproductivity restoration in a part of the Aral Sea.

Possible ways for rehabilitation of the Aral Sea are as follows:

- Reducing up to 70 % of the Amu-Darya water for irrigation, which would increase the Aral Sea level up to 38.5 m (an unrealistic version);
- Separation of the Western and Eastern parts and keeping only one of them with 20–35 % reduction of water for irrigation.

In this paper, some results of the numerical modeling of the Aral Sea circulation as well as demineralization during a high-water period of 1998 are presented. The 3D model used in the numerical experiment is the Novosibirsk Computing Center (now the ICM&MG) ocean circulation model [1–3] adapted to the Aral Sea basin.

---

\*Supported by INTAS Grant 2001-0511-REBASOWS.

## 1. A three-dimensional hydrodynamic model of hydrophysical processes in the Aral Sea

There are two versions of the Aral Sea circulation model in Laboratory of Mathematical Modeling of the Hydrosphere ICM&MG SD RAS, which were adopted from the basic circulation models for investigation in the ocean and in the marginal seas.

The general features of the models are the following:

- Mathematical model is based on the complete “primitive” nonlinear equations of the thermo-hydrodynamics of the ocean;
- Temperature and salinity distributions are calculated;
- The models have a possibility to include the calculation of the pollutants;
- The interaction with the atmosphere is realized via the upper mixed layer with the possibility to include the ice formation;
- The models have a possibility to include the inflows and outflows from the basin;
- The models are based on a combination of the finite element and the splitting methods;
- The triangulated quasi-regular B-grid is used in the model;
- The models differ in the method of the vertical levels distribution: sigma-coordinate model and  $z$ -coordinate model.

### 1.1. The input and the output of the model

**The input of the model:** At the sea surface:

- Wind-stress calculated by the wind at 2 m height;
- Temperature, salinity (fresh water) fluxes.

At the inflow lateral boundaries:

- Fresh water mass flux (the river inflow);
- Temperature and salinity prescribed.

Initial state: Temperature, salinity climatic 3D distribution.

**The output of the model:**

- 3D velocity field;
- Temperature and salinity fields in the seasonal cycle.

**Data sources:**

- Meteorological data for the calculations of the temperature and salinity fluxes;
- The Amu-Darya river runoff;
- The NCEP/NCAR reanalysis wind for the wind-stress calculation.

**1.2. Designing the experiments and analysis of the results**

The Aral Sea region for calculation of the 3D currents, thermodynamics as well as spreading of the fresh water is constructed on the basis of the bottom topography produced by the Uzbekistan colleagues. The level of 32.5 m is set as the initial value for the determination of the basin area. The bottom topography is presented in Figure 1.

An essential difference in the bottom relief of the Western and the Eastern parts of the Aral Sea causes some difficulties in the modeling on the unique version of the vertical grid. The cross-section across the basin along the latitude is presented in Figure 2a. Because of this reason, in the Western Part of the Sea where a maximum value of the depth is 48 m,  $z$ -coordinate

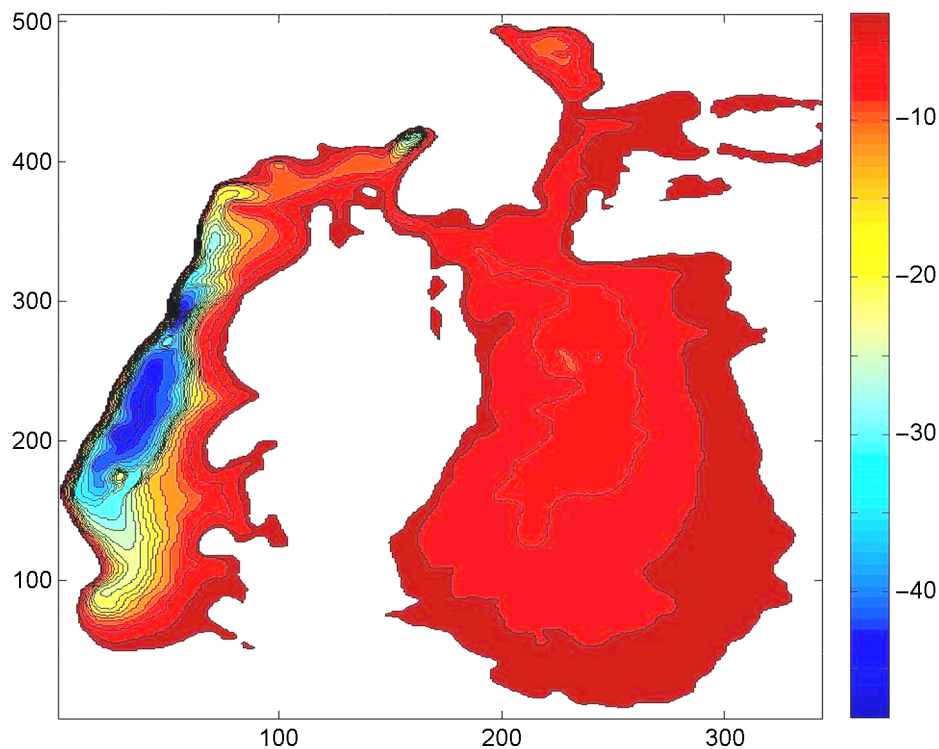


**Figure 1.** The levels of height (Baltic system) for Aral Sea basin in meters

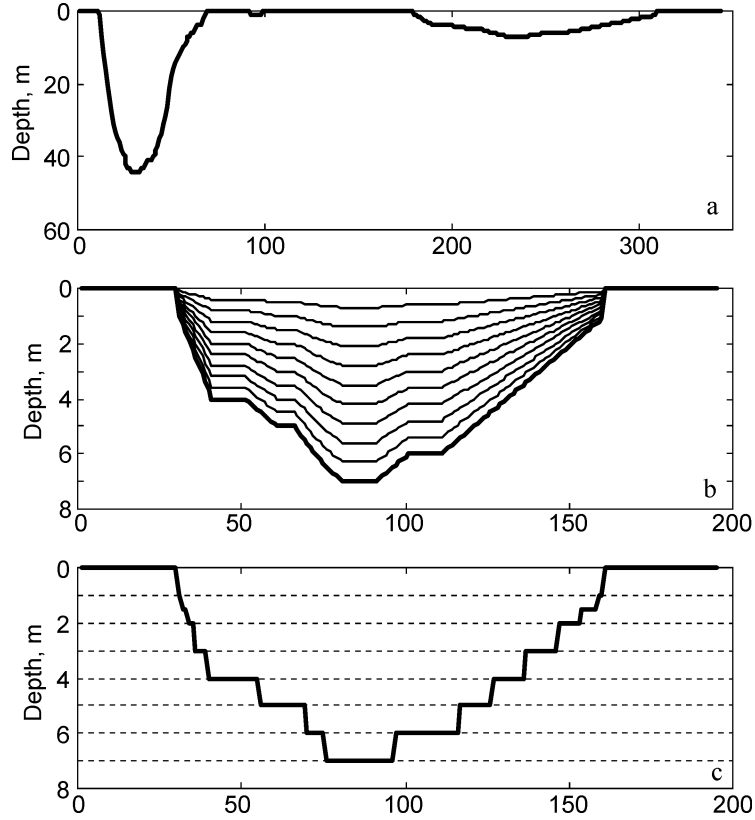


**Figure 2.** The vertical cross-section of Aral Sea along the latitude (a); schematic representation of sigma-coordinate (b) and  $z$ -coordinate (c) grids

multilevel model is more preferable. The sigma-coordinate model was used for the Eastern Part of the Aral basin with a weakly changing depth with a maximum value of 14 m. The schematic representation of the two coordinate systems in the model is shown in Figures 2b and 2c. The two coordinate systems were connected on the basis of the domain decomposition technology.

The numerical model has  $1000 \times 1000$  m horizontal grid resolution, which corresponds to the array with  $86 \times 195$  nodes. By the vertical, a nonuniform grid is used (35 levels for a maximum depth). In the regions with a minimum depth of 2 m, five levels are included. The vertical grid has the following levels:

$$\begin{aligned}
 Z = & 0, 0.5, 1, 1.5, 2, 3, 4, 5, 6, 7, 8, 9, 10, \\
 & 11, 12, 13, 14, 15, 17, 19, 21, 23, 25, 27, \\
 & 29, 31, 33, 35, 37, 39, 41, 43, 45, 47.
 \end{aligned}$$

## 2. Numerical experiments

### 2.1. The first experiment

At the first stage of the numerical experiment, the Aral Sea basin was taken in a total configuration without dam between the Eastern and the Western parts. The Amu-Darya river runoff was directed to the Eastern part.

At the initial stage, we had no spatial distribution of the climatic data. So, the constant values of the temperature (25 °C) and salinity (68 g/l) corresponding to the summer season were set in the whole basin. The integration of the model was carried out during the period of about two years with the wind-stress produced from the NCEP/NCAR wind. The time step was one hour. On each step, the following 3D hydrophysical fields were calculated: temperature, salinity, velocity and fresh water as a tracer.

The results of the numerical experiment allow us obtain some specific features of the Aral Sea circulation, thermodynamics and fresh water spreading.

**The circulation** in the Aral Sea basin is highly varying, and although there are no strongly dominating pictures of the main circulation, it is possible to distinguish some specific features.

First, the circulation is very sensitive to the wind and is mainly derived by the wind, except a short period of the ice covering the sea surface. The Eastern part is very shallow and has the fastest feedback to the wind change. A wide area of the Eastern part allows a well-manifested cyclonic (Figures 3, 4) or anticyclonic (Figure 5) circulation to be formed. The transition period between them is characterized by the dipole circulation (Figures 6, 7). The Western basin is narrower and deeper. So, the circulation consists of more local gyres, but the feedback to the wind change is slower than the one of the Eastern basin.

The circulation variations during the seasons of the integration period may roughly be described in the following way. In the summer period, in the Eastern part, there was a cyclonic circulation. In Figures 3, 4, the integral stream function as well as the velocity field at a depth of 2 m are presented. The velocity value attains 30 cm/s. The circulation in the Western basin is cyclonic in the South and anticyclonic in the North. There also exist some local circulations caused by the bottom topography and the basin configuration. During the winter period, when the wind is blocked by the ice cover, this circulation is weakening (Figure 8), until the ice cover disappears. In spring, the reconstruction of the circulation in some periods leads to a sufficiently chaotic circulation, becoming stable enough by May.

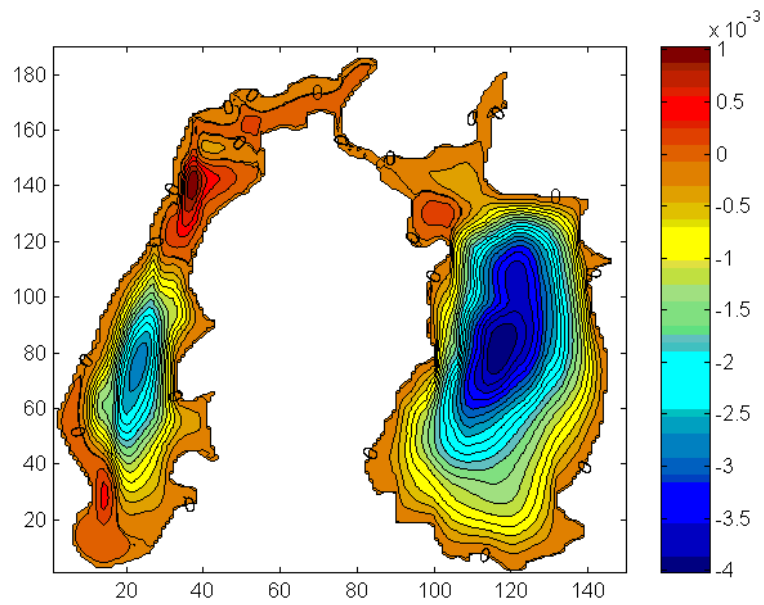


Figure 3. Stream function, June

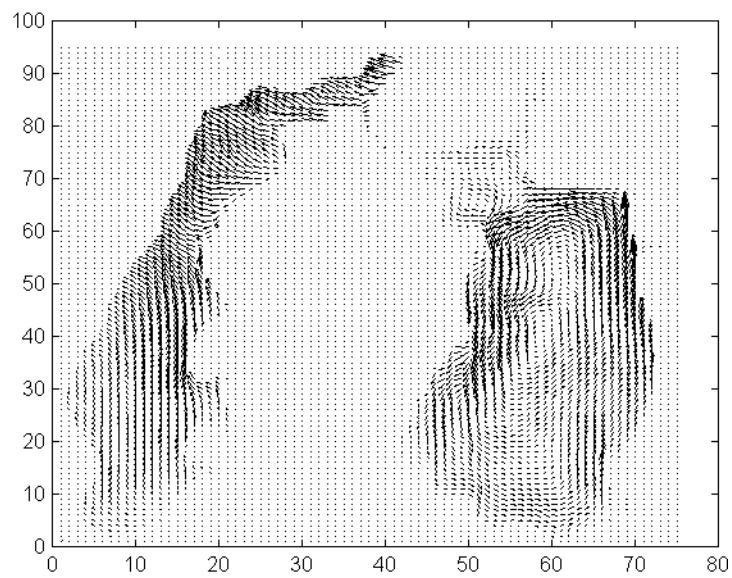


Figure 4. Velocity field at a depth of 2 m, June

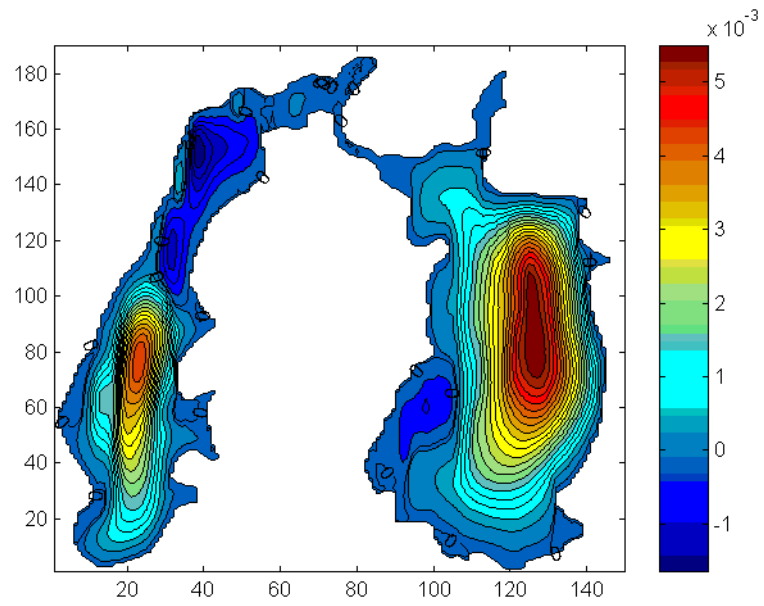


Figure 5. Stream function, January

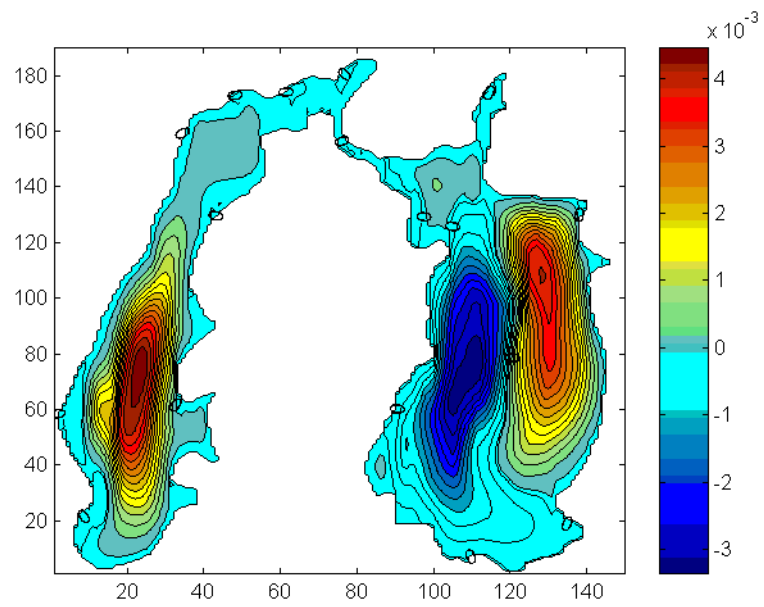
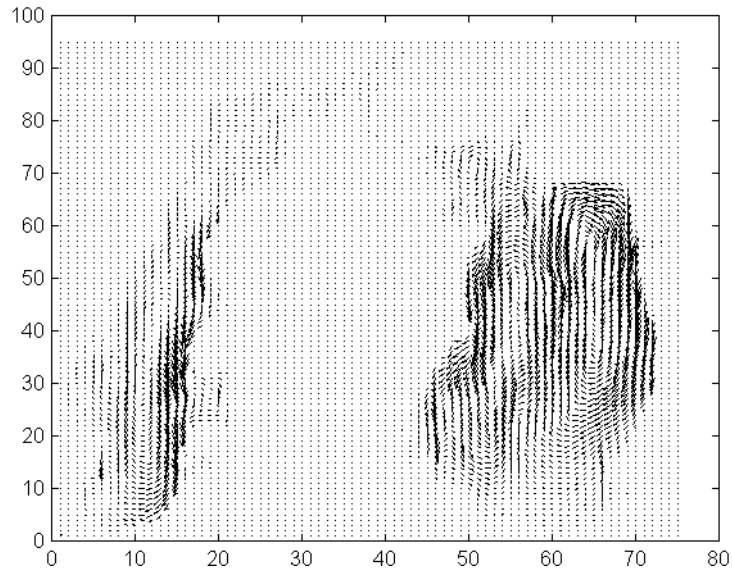
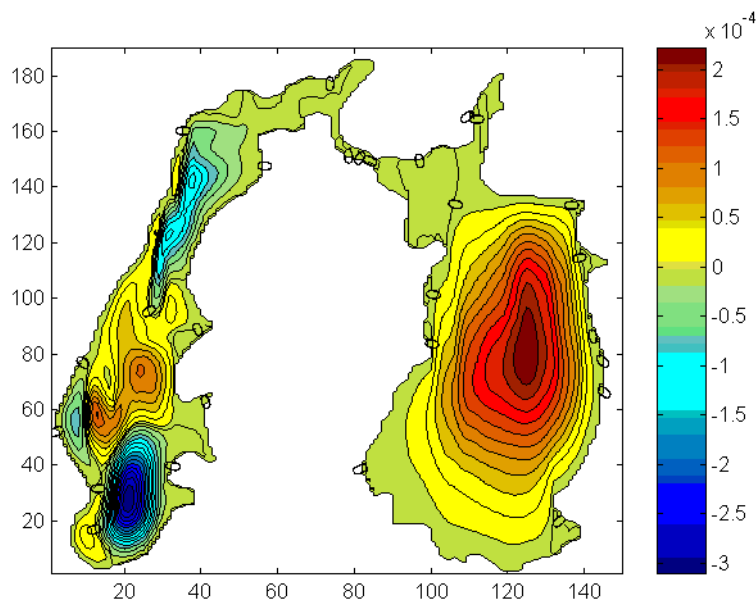


Figure 6. Stream function, December



**Figure 7.** Velocity field at a depth of 2 m, December



**Figure 8.** Stream function, February

**The thermodynamics.** The seasonal variations of the Aral Sea are influenced by the seasonal cycle, but the processes of the seasonal variations in the Western and the Eastern parts are different.

In the Eastern part, the temperature is determined by the heating and cooling processes on the surface and the mixing by wind. This brings about a homogeneous distribution of temperature in the Eastern part within the range from 0 to 27°C.

In contrast to this, the result of the calculations shows that the thermal conditions of the Western part of the Aral Sea, determined by a seasonal cycle are divided into two main states: summer stratification and winter homothermy. The summer distribution has the temperature stratification of about 20 degrees, with a strong thermocline, which is well manifested in Figure 9.

The horizontal distribution is characterized by the lower temperature values in the western deep part and higher values in the eastern part (Figure 10). Cooling in the autumn and the winter seasons results in the density convection and the homothermy. In Figure 11, one can see the convection in the Western part of the basin. The upper layer is completely mixed, whereas more saline and denser water in the deeper layer prevents mixing. Nevertheless, finally, the vertical temperature distribution has become homogenous.

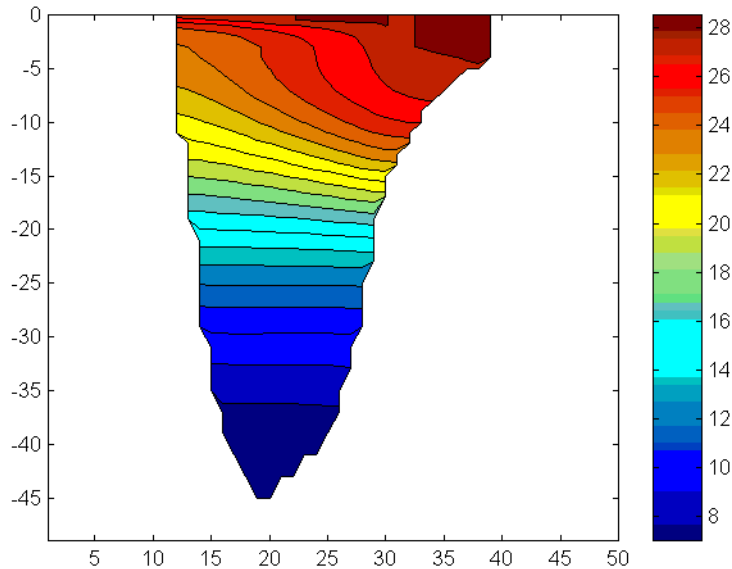


**Figure 9.** Latitudinal temperature cross-section.  
Western basin. Summer

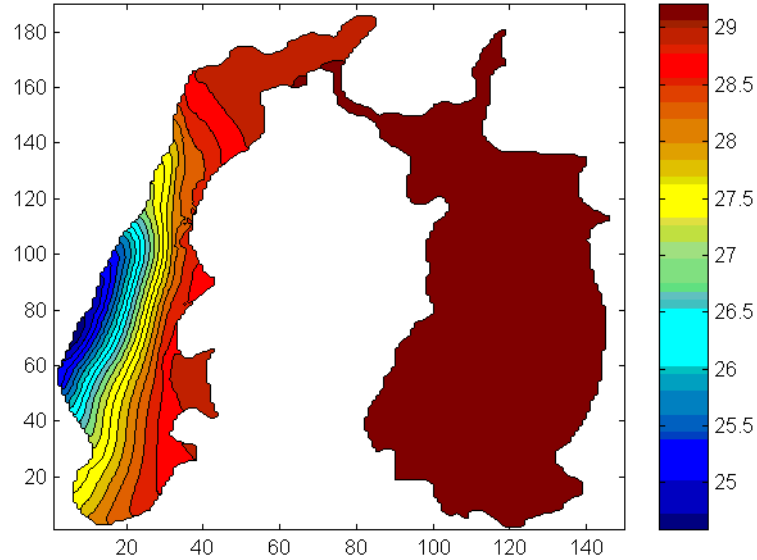


**Figure 10.** Temperature at a depth of 2 m, June

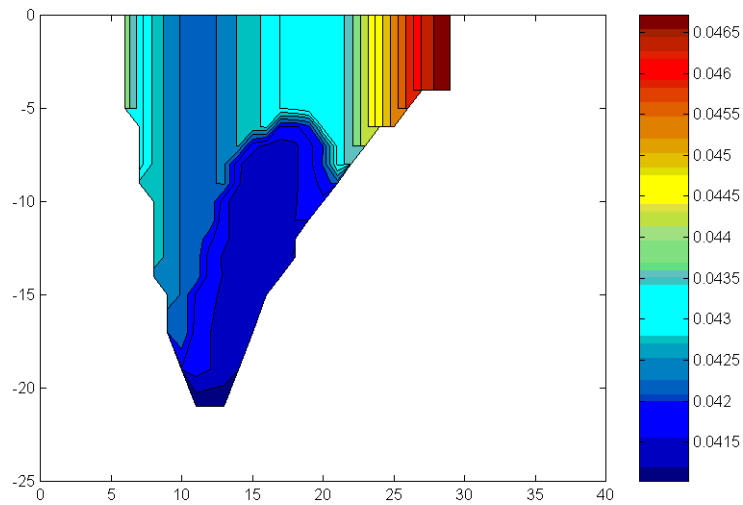


**Figure 11.** Latitudinal temperature cross-section near the river inflow, Winter

**The salinity distribution and the fresh water propagation.** The salinity conditions during the integration period are defined by the Amu-Darya inflow during May-September, 1998. In this period, the river inflow was extremely high. The pictures present the propagation of the fresh water through the Eastern basin. In Figure 12, the horizontal picture before refreshing is presented. In Figure 13, the horizontal salinity distribution during the period of the refreshing are presented.

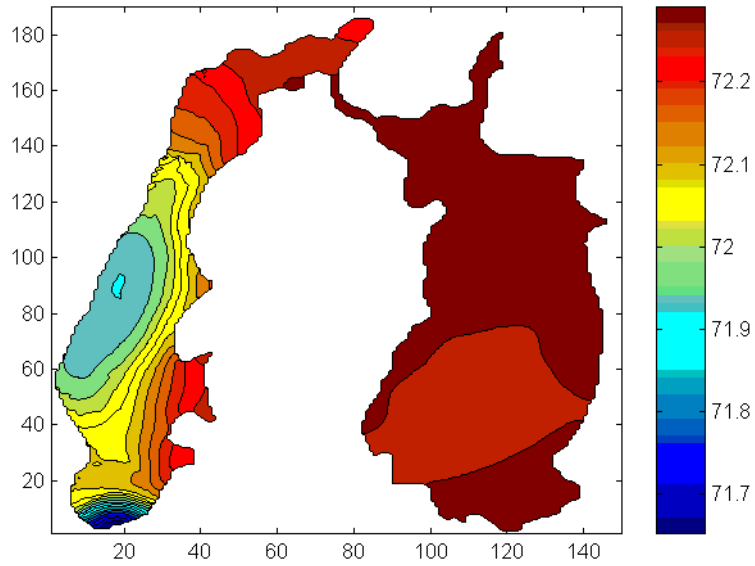


Figure 12. Salinity field at a depth of 6 m, Summer

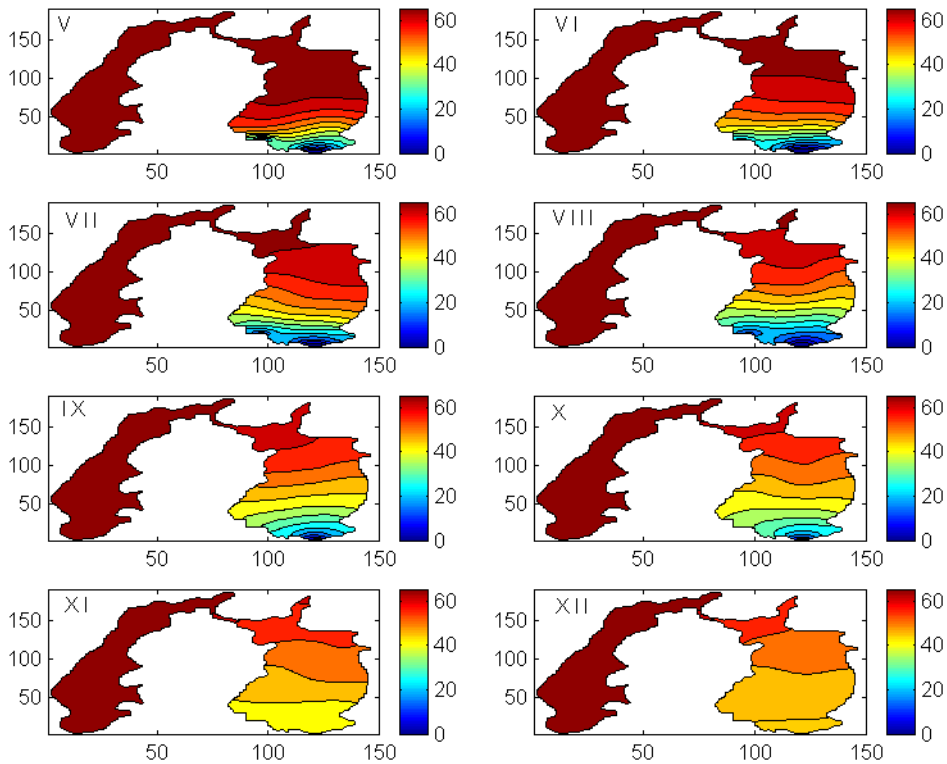
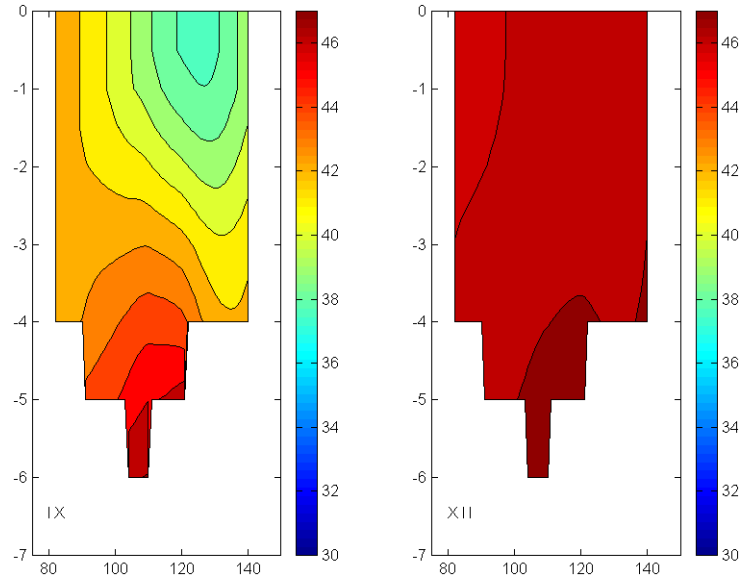
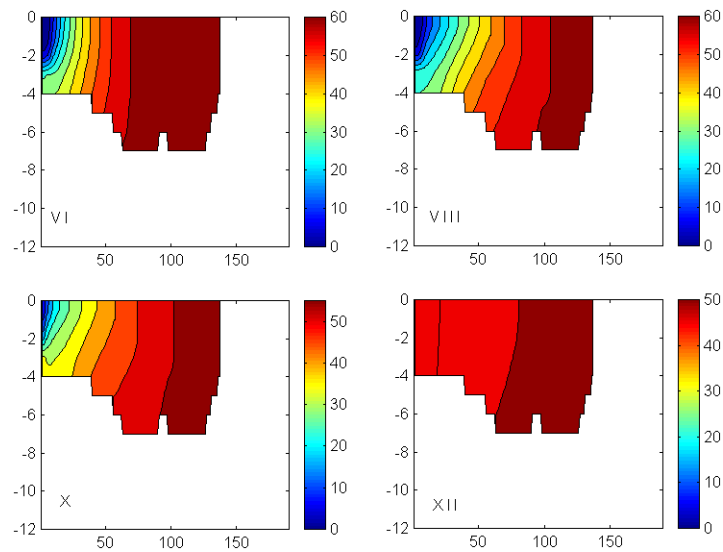


Figure 13. Desalination of the Aral Sea during the period of V–IX 1998 – a high Amu-Darya inflow and of X–XII 1998 – a low Amu-Darya inflow



**Figure 14.** Latitudinal salinity cross-section for September and December 1998



**Figure 15.** Meridional salinity cross-section for June, August, October, December 1998

After the river inflow stops, the horizontal distribution becomes nearly uniform, but the salinity is lower than that at the initial moment. One can see a well-manifested movement of the low saline water from South to North. The pool of the freshened water has a tendency to turn to the East under the influence of the circulation (Figures 13–15). The fresh water reaches a

narrow straight between the Eastern and the Western parts of the basins and propagates to the Northern part of the Western basin.

## 2.2. The second experiment

At the second stage of the numerical experiment, the Aral Sea basin was taken in a configuration with a dam between the Eastern and the Western parts as compared to the first experiment. The Amu-Darya river runoff was directed to the Western part.

The circulation is also derived mainly by the wind-stress and influenced by the bottom topography and configuration of the basin and is very similar to that of the first experiment. In Figures 16, 17, the horizontal velocity fields at depths of 3 m and 9 m are presented, respectively.

In this case the spreading of the fresh water is restricted by the dam and does not come to the Eastern basin. This leads to a stronger refreshing of the Western basin. The main difference is concentrated in the salinity field because of the fresh water inflow to the Southern part of the Western basin. The fresh water propagates from South and after the period of integration comes to the North of the basin. The salinity distribution is presented in Figure 18. The vertical cross-section along the longitude from the river inflow up to the coast is presented in Figure 19. One can see that the fresh water comes not by the surface but along the middle layer at a depth of about 15 meters.

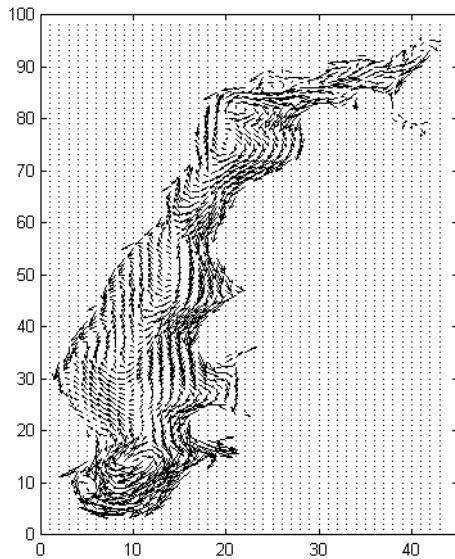


**Figure 16.** Velocity field at a depth of 3 m. Maximum velocity 20 cm/s

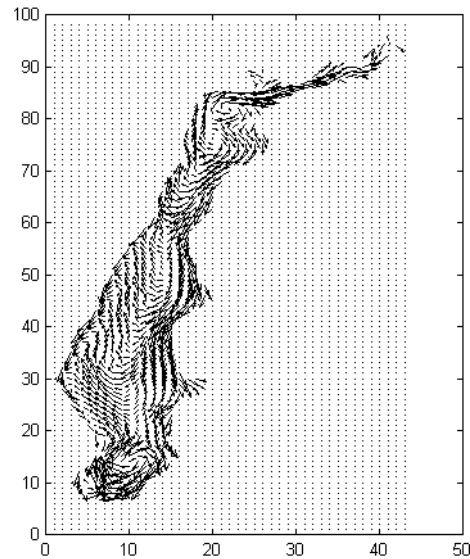


**Figure 17.** Velocity field at a depth of 9 m. Maximum velocity 9 cm/s

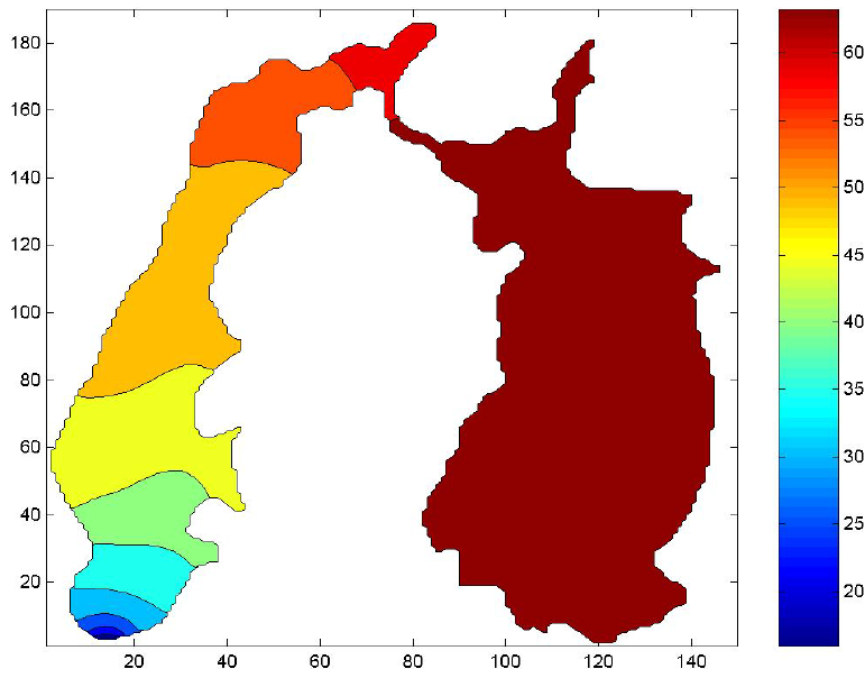


**Figure 18.** Salinity distribution at a depth of 7 m after two years

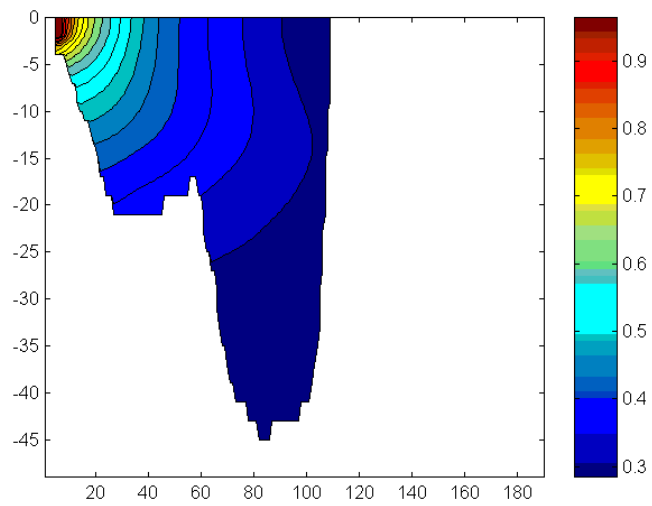


**Figure 19.** Fresh water distribution (in abstract units).  
The vertical cross-section near the river inflow

## **References**

- [1] Kuzin V.I. Finite Element Method in the Modeling of the Ocean Processes. — Novosibirsk: NCC Publisher, 1986 (In Russian).
- [2] Kuzin V.I. The ocean circulation models on the on the finite element method with the splitting // *Vychislitel'nye Protsessy i Sistemy*. — 1986. — Vol. 4. — P. 105–122 (In Russian).
- [3] Golubeva E.N., Ivanov Ju.A., Kuzin V.I., Platov G.A. Numerical modeling of the World Ocean circulation including upper ocean mixed layer // *Oceanology*. — 1992. — Vol. 32. — No. 3. — P. 395–405.

